Tropical aerosol in the Aleutian High

V. Lynn Harvey,[1] Matthew H. Hitchman,[2] R. Bradley Pierce,[3] and
T. Duncan Fairlie[4]

Abstract. Stratospheric aerosol profiles at high northern latitudes from the Stratospheric Aerosol Measurement (SAM) II experiment are used to document the aerosol maxima that occur in the major wintertime anticyclones. Fourteen years (1978–1991) of 1 μm extinction are used to calculate median values for each season in bins of 5° latitude by 30° longitude by 1 km altitude. Longitude-altitude sections of estimated surface area density show that tropical, aerosol rich air tends to accumulate in the Aleutian High from 15 to above 30 km, and in the North Atlantic High in the 15–25 km layer. A trajectory case study with winds from the European Center for Medium-Range Weather Forecasting is used to investigate the hypothesis that the observed aerosol maxima are maintained by episodic poleward surges of high aerosol air from the tropical stratospheric reservoir. Lagrangian trajectories are initialized and run backward in time, from both a high-resolution grid and SAM II occultations, for selected days when high aerosol is found in the Aleutian High. Results show that during the case study provided, a deep sheet of aerosol rich air originating over Africa is advected poleward and eastward around the polar vortex and entrained into the Aleutian High.

1. Introduction

It is well accepted that air predominantly enters the stratosphere in the tropics [*Brewer, 1949; Mote et al.*, 1996] and descends back into the troposphere at high latitudes [*Holton et al.*, 1995], notably through the winter polar vortices [*Schoeberl et al.*, 1992; *Manney et al.*, 1994] and in tropopause folding events [*Danielsen*, 1968; *Shapiro et al.*, 1984; *Hamill et al.*, 1997; *Postel and Hitchman*, 1998]. The hemispheric poleward and downward Brewer-Dobson circulation in the middle and lower stratosphere is apparent in zonal mean tracer distributions where isopleths are lofted in the tropics and depressed at higher latitudes [e.g., *Kumer et al.*, 1993]. Much evidence points to the tropical middle stratosphere being somewhat sequestered from the vigorous stirring processes associated with extratropical waves [*Murphy et al.*, 1993; *McCormick and Veiga*, 1992; *Trepte and Hitchman*, 1992; *Randel et al.*, 1993; *Grant et al.*, 1996], with the steep subtropical constituent gradients suggesting a tropical stratospheric reservoir (TSR) [*Hitchman et al.*, 1994]. Aerosol is observed to maximize in the TSR [*Hitchman et al.*, 1994]. Processes that contribute toward the tropical aerosol maximum include preferential heteromolecular homogeneous nucleation of sulfuric acid and water at the cold tropical tropopause [*Hamill et al.*, 1997] differential vertical motion, and rapid poleward and downward transport out of the extratropical lower stratosphere [*Trepte et al.*, 1993]. The latter two processes, together with two-way mixing across the subtropics, can account for why a large volcanic eruption at nearly any location leads to a tropical relative maximum several months later [*Hitchman et al.*, 1994]. Benefits of studying the quasi-horizontal mixing between the TSR and the midlatitudes include the effects of tropical chemical constituents on the extratropical ozone distribution and, conversely, the influence of midlatitude pollutants entrained into the TSR [*Stolarski et al.*, 1995].

Leovy et al. [1985] were perhaps the first to use global satellite constituent data to depict the manner in which stratospheric air departs the TSR: high tropical ozone surges poleward in synoptic scale "tongues" of air. Subsequent satellite constituent studies of this phenomenon include *Randel et al.* [1993], *Manney et al.* [1993], *Trepte et al.* [1993], *Manney et al.*, [1995a], *Lambert et al.*, 1996, and *Rogers et al.* [1998]. Other recent observational work used meridional excursions of constant-level balloons [*Rom-Kedar and Paldor*, 1997]. Numerical model simulations [*Rood et al.*, 1992; *Chen et al.*, 1994; *Fairlie*, 1995; *Orsolini*, 1995] and trajectory studies [*Norton*, 1994; *Pierce et al.*, 1994; *Waugh et al.*, 1994; *Schoeberl and Newman*, 1995; *Manney et al.*, 1995b] also provide convincing evidence of sporadic poleward transport from the TSR, beginning in the subtropics where large meridional tracer gradients are observed.

These surge events are highly variable in space and time. The magnitude of transport from the TSR to midlatitudes is greatest in the winter hemisphere and depends on altitude [*Chen et al.*, 1994; *Hitchman et al.*, 1994; *Langford et al.*, 1995; *Waugh*, 1996]. The vertical dependence has been described in terms of a "lower transport regime" and an "upper transport regime" [*Trepte and Hitchman*, 1992]. In the lower transport regime (within about 5 km of the tropopause), air is readily transported poleward in association with upwardly evanescent tropospheric disturbances. In situ tracer data indicate significant exchange between the TSR and the midlatitudes at timescales of months and longer. *Volk et al.* [1996], *Minschwaner et al.* [1996], and *Avallone and Prather* [1996] estimated that 50% of air in the TSR at 21 km is of midlatitude origin. The upper stratospheric transport regime (21–28 km) is characterized by

[1] Science Applications International Corporation, Hampton, Virginia.
[2] Department of Atmospheric and Oceanic Sciences, University of Wisconsin, Madison, Wisconsin.
[3] NASA Langley Research Center, Hampton, Virginia.
[4] Science and Technology Corporation, Hampton, Virginia.

episodic poleward transport events which can be modulated by the Quasi-Biennial Oscillation (QBO) [*Trepte and Hitchman*, 1992; *Grant et al.*, 1996; *O'Sullivan and Dunkerton*, 1997; *Schoeberl et al.*, 1997]. This study focuses on transport in the upper regime. At higher altitudes, transport from the tropics to midlatitudes is observed as discrete events where planetary scale "tongues" of tropical tracers mix irreversibly poleward. These large poleward excursions in the middle to upper stratosphere may be induced when the polar vortex is displaced equatorward [*Waugh*, 1993]. This can occur when the Aleutian High (AH) is amplified, suggesting self-maintenance via vortex-vortex interaction [*O'Neill et al.*, 1994; *Harvey and Hitchman*, 1996]. Other studies suggest that weak inertial instability associated with poleward motion of low potential vorticity and anticyclogenesis is a significant mechanism by which air begins to surge poleward [*O'Sullivan and Hitchman*, 1992; *Knox*, 1996; *Orsolini et al.*, 1997; *Mecikalski and Tripoli*, 1998].

It remains to determine where the tropical air in these surge events ends up, whether it tends to accumulate in specific regions or be distributed fairly uniformly throughout middle latitudes. While it is generally agreed that mixing across the edge of the polar vortex is small in the upper and middle stratosphere [*Pierce and Fairlie*, 1993], mixing across the vortex edge increases in the lower stratosphere (450 K) [*Dahlberg and Bowman*, 1994], and tropical intrusions can penetrate to the core of the polar vortex [*Plumb et al.*, 1994]. Aerosol that has been transported from the TSR to midlatitudes has been later observed in the Arctic polar vortex [*Rosen et al.*, 1992; *Bormann et al.*, 1993] where it can affect the ozone budget through heterogeneous reactions [*Hofmann and Oltmans*, 1993]. However, entrainment of tropical aerosol rich air into the polar vortex is slow in the middle stratosphere. In addition, the size of the AH nearly always increases in the days following poleward surge events. Here we follow reasoning in previous work and explore the idea that this tropical air commonly gets entrained into the AH [*Waugh*, 1993; *Lahoz et al.*, 1994; *O'Neill et al.*, 1994; *Manney et al.*, 1995a, b; *Polvani et al.*, 1995; *Fairlie*, 1995]. In this paper we establish a connection between the repeated injection of tropical high aerosol air into the AH and the climatological high aerosol observed in the AH during northern winter.

This paper is organized as follows: Section 2 describes the SAM II data, the European Centre for Medium-Range Weather Forecasting (ECMWF) analyses, and construction of the SAM II aerosol climatology. In section 3, longitude-altitude sections show high aerosol in the AH during the December-January-February (DJF) season. The variability of aerosol surface area density (SAD) is greater in the anticyclones compared with that in the polar vortex. In order to identify the origin of the high aerosol in the AH a case study is presented in section 4 in which Lagrangian back trajectories are initialized from a 0.5° by 0.5° grid and from SAM II occultations on a day when the satellite measured high aerosol in the AH. A tropical source for the high aerosol over Africa is identified. The three-dimensional structure of the aerosol rich air mass is shown to be a deep sheet of tropical air (extending over 5 km) which is entrained poleward and eastward around the polar vortex and into the AH. Conclusions are given in section 5.

2. Data and Analysis

The SAM II sensor is a Sun photometer mounted on the Nimbus-7 spacecraft which measures attenuated sunlight at 1 μm through the atmospheric limb at each satellite sunrise and sunset. It orbits the Earth in 90 min, taking 15 limb soundings per day near both poles, with the sampled latitude sweeping from ~65° to 85° in about 3 months. Each vertical sounding begins at 30 km and extends down to the surface with 1 km resolution, unless a cloud is encountered. The data record extends from October 24, 1978 to December 5, 1992. Care must be used with sunset data in the Northern Hemisphere taken after January 1990 when the instrument's view of the Sun became obscured by a nearby antenna. A more detailed discussion of the SAM II instrument and data is given by *McCormick et al.* [1979] and *Russell et al.* [1981].

A three-dimensional, SAM II aerosol climatology was created by binning 1 μm extinction values into 5° latitude, 30° longitude, 1 km altitude for each season. The bin size is constrained by the 26° longitudinal sampling frequency of the SAM II instrument. While this coarse spatial sampling does not capture small-scale structure such as filaments, large-scale stratospheric features are resolved by the SAM II data. The spatial domain of the climatology is limited to high latitudes, extending from 65° to 85° in either hemisphere and from 30 km down to the extratropical tropopause (typically 8–9 km). Below 25 km the estimated extinction error is typically less than 10%. Above this altitude it is common for the error to exceed 50%. Therefore extinction values with estimated errors larger than 50% were not included. There were more than 100 samples per bin from 10 to 25 km and more than 200 from 13 to 21 km. Above 25 km this number decreased rapidly. Seasonal median values of extinction were calculated for each bin and converted to SAD using equation (5) of *Thomason et al.* [1997]. Medians were used instead of averages to ensure that the climatology was not skewed by sporadic observations of elevated extinction which occur following volcanic eruptions or when polar stratospheric clouds (PSC) are sampled. SAD values were generally represented by a lognormal distribution. However, long tails of large SAD values were observed in some bins. In order to filter these values from the climatology we performed five iterations on the median whereby outlying aerosol values greater than four standard deviations away from the previous median were excluded. Effects of filtering in this manner were maximized in the 15–20 km layer in the anticyclones where the number of observations per bin decreased by more than 30. Climatological SAD values were reduced by 15% in these regions. Surprisingly, the filter had very little effect in the north polar vortex. No other attempt was made to clear clouds, hence care should be used in interpretation of results where temperatures are cold enough to form PSCs. In the Arctic the likelihood of encountering a PSC maximizes at 10% of the time in early February, in the layer 20–22 km, from 90°W through the Greenwich meridian to 90°E [*Poole and Pitts*, 1994]. The zonal mean seasonal structures of SAD (not shown) are consistent with previous two-dimensional analyses [e.g., *Hitchman et al.*, 1994; *Thomason et al.*, 1997].

The ECMWF data used in this study are uninitialized analyses with 2.5° resolution in latitude and longitude. Geopotential height, temperature, relative humidity, and winds were obtained from the National Center for Atmospheric Research (NCAR) on the following 14 pressure surfaces: 1000, 850, 700, 600, 500, 300, 250, 200, 150, 100, 70, 50, 30, and 10 hPa. *Trenberth* [1992] provides a discussion of the observation types, assimilation methods, and data quality for the ECMWF products.
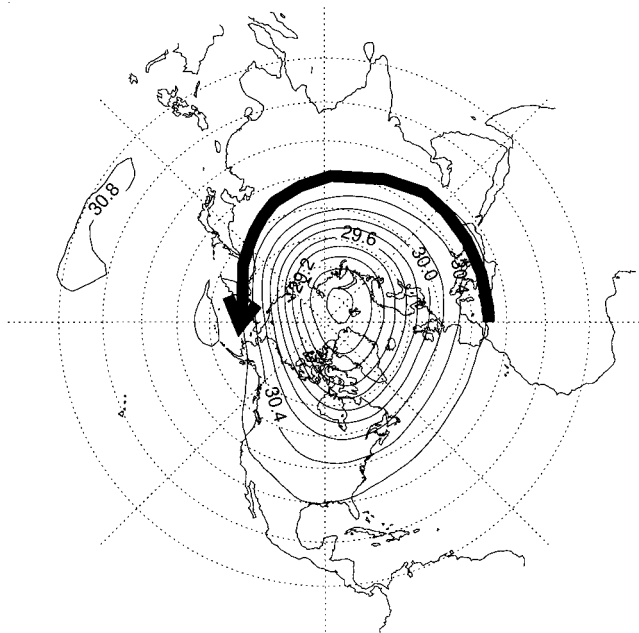
Figure 1. Northern Hemisphere polar stereographic projection of 1985–1991 DJF average geopotential height at 10 hPa (in kilometers). Contour interval is 200 m. The arrow follows the 30.6 km geopotential height contour from the Greenwich meridian (GM) to the date line.

3. Climatological Structure

Figure 1 shows the 6-year (1986–1991) average DJF geopotential height at 10 hPa. The climatological polar vortex center is displaced into the eastern hemisphere, with trough elongation over eastern North America and central Asia at this level. The AH is centered near 50°N and the date line. The arrow illustrates the climatological pathway where tropical air is transported poleward. From geostrophic considerations alone, air that originates near North Africa will follow geopotential height contours eastward around the polar vortex and poleward to 60°N at the date line. This transport pattern is observed in the ECMWF analyses on a daily basis in the form of mobile anticyclones, which originate in the vicinity of the Greenwich meridian (GM) (at 10 hPa) and propagate eastward around the polar vortex along this pathway [*Harvey*, 1994; *O'Neill et al.*, 1994]. Tropical air that follows this path could be entrained into the AH.

Figure 2 is a longitude-altitude section at 65°N of the DJF averaged geopotential height, where the zonal mean has been subtracted. Henceforth eddy refers to deviations from the zonal mean. Positive eddy heights at the date line denote the AH. Negative eddy heights, which tilt westward with altitude from 140°W near 250 hPa, denote the polar vortex. The "North Atlantic High" (NAH) is visible as high values centered at the GM in the lower stratosphere but decays with altitude.

Figure 3 shows the corresponding longitude-altitude section of SAM II DJF median aerosol SAD near 65°N (expressed as a % departure from the zonal mean). At this latitude, SAM II makes continuous observations both inside the AH and in the Arctic polar vortex. By comparing Figures 2 and 3 it is immediately apparent that above 15 km, high aerosol SAD is coincident with the AH and the NAH, while low aerosol SAD is found in the polar vortex. Between 15 and 30 km an increase
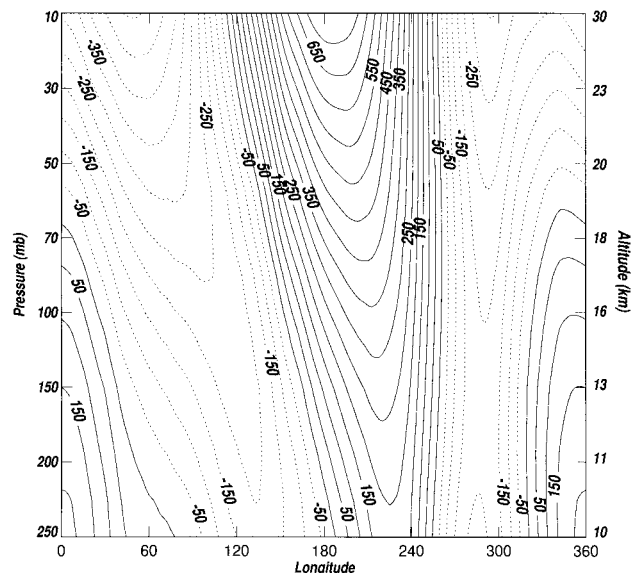

Figure 2. Longitude-altitude section at 65°N of 1985–1991 DJF average eddy geopotential height (deviation from the zonal mean, in meters). Contour interval is 50 m.

in aerosol of up to 25% over the zonal mean is observed in the AH. From 10 to 25 km the NAH shows an increase of up to 20%. Air in the polar vortex shows up to a 30% reduction in zonal mean SAD. Absolute SAD values can be calculated from the zonal mean profile given to the right of Figure 3. Horizontal lines show plus and minus 1 standard deviation from the zonal mean at each level. Previous aerosol observations by SAM II [*Kent et al.*, 1985] and LIDAR [*Dameris et al.*, 1995] also show aerosol poor air inside the Arctic polar vortex at these altitudes. This climatological wintertime structure of aerosol in longitude at 65°N is consistent with observed longi-
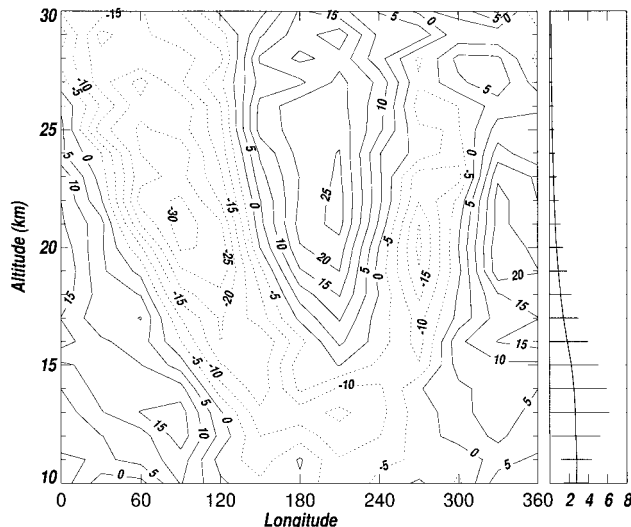

Figure 3. Longitude-altitude section at 65°N of 1978–1991 DJF SAM II surface area density expressed as a percent deviation from the zonal mean. Contour interval is 5%. Zonal mean SAD profile given to the right in units of μm^2 cm^{-3}. Horizontal lines show, plus and minus 1 standard deviation from the zonal mean at each level.
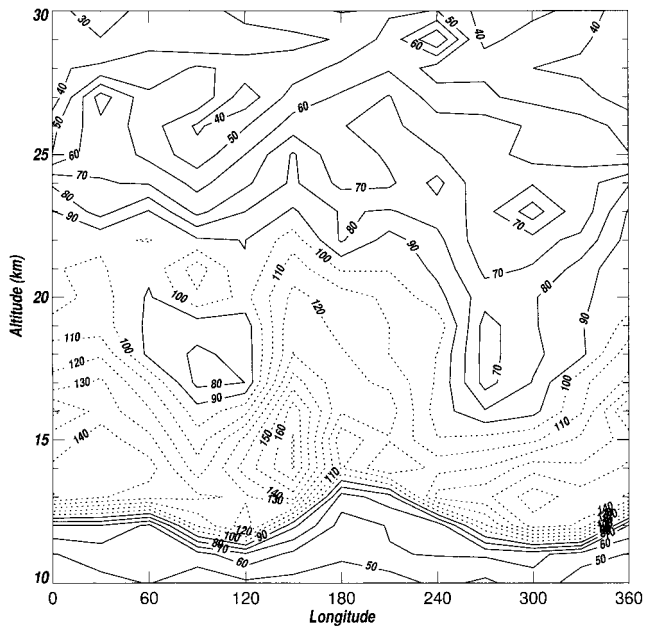
Figure 4. Longitude-altitude section at 65°N of the standard deviation of the surface area density climatology expressed as percent of the SAD climatology. Contour interval is 10%. Values greater than 100 are dashed.

tudinal variations of daily water vapor, nitrous oxide, and methane from 20 to 40 km, at latitudes where sampling occurs both inside and outside of the polar vortex [*Lahoz et al.*, 1993; *Ziemke and Stanford*, 1995].

Figure 4 is the standard deviation of the SAD climatology shown in Figure 3 expressed as a percent of the SAD climatology. This shows the temporal variability about the aerosol climatology in terms of a percent. Values greater than 100 (where the standard deviation is equal to the climatological SAD value) are dashed. Variability is greatest in the lower stratosphere and is particularly large near 15 km in the polar vortex, possibly reflecting PSC variability. Elsewhere, variability tends to be larger in the anticyclones. This result is consistent with the notion that high aerosol air is intermittently injected into the anticyclones, while the polar vortex remains relatively clean. Vascillating between sampling inside and then outside of the polar vortex at 65°N may also contribute to regions of high variability.

4. Poleward Surge Case Study

Previous work has shown that tropical middle stratospheric air, identified by its warm temperatures, low potential vorticity, and signature of high aerosol, surges poleward in robust, episodic wave events. Poleward surges typically occur every couple of weeks in the middle stratosphere; however, some winter months have none, while others have three or four. Here we explore this possible mechanism for establishing the elevated aerosol levels observed in the AH. To define the current case study, we first identified days when SAM II sampled both inside the polar vortex and in the AH. From there we chose days where the daily aerosol structure in longitude resembled that in the climatology (see Figure 3). When SAM II samples both in the polar vortex and in the AH, this aerosol structure is common. On days that satisfied both of these criteria we

initialized trajectories from the SAM II soundings and ran them backward in time to identify the origin of the high aerosol. During the winter of 1985–1986, about one surge per month was observed. The strength of the polar vortex during the winter of 1985–1986 was not unusual. However, this winter was dynamically active in terms of anticyclogenesis. From late November to February both the AH and the NAH were strong and persistent [*Harvey and Hitchman*, 1996, Figure 2]. The phase of the QBO was easterly, consistent with a "disturbed" polar vortex [*Holton and Tan*, 1980]. We include only one case study because it is representative of the four or five surges that occurred this winter. It is also similar to poleward surge events observed during other winters. In late January 1986 the AH was well defined and quasi-stationary, and SAM II consistently made measurements (at 69°N) both inside the AH and in the polar vortex. January 23 was chosen as the first day of the case study. During the week, preceding this date, there was a surge of tropical air into midlatitudes. This was seen as a mobile anticyclone that developed near the GM at 10 hPa, propagated eastward around the polar vortex, and merged with the AH. A well-defined, quasi-stationary AH persisted over the Aleutian Islands for 3 weeks following this surge event.

Figures 5a and 5b show northern hemisphere fields of Montgomery stream function ($M = c_p T + gZ$) and pressure at 700 K on January 23, respectively. M is the isentropic analog to the geopotential height shown in Figure 1 and illustrates the circulation pattern on this day. Air flows approximately parallel to the contours of M on an isentropic surface (Figure 5a) such that under steady conditions, a parcel starting at 40°N and the GM would be advected poleward to 70°N at the date line. This is a direct result of the presence of the AH. Notice the weak anticyclone over Africa in the M field. Figure 5b shows that the height of the 700 K surface undulates 15 hPa in altitude (over 4 km). It peaks over Greenland, at 12 hPa, in association with the cold polar vortex and is lowest, at 27 hPa, to the west of the AH where the warmest temperatures are observed. Considering Figures 5a and 5b together show how air in the confluent polar jet over the Bering Sea descends and splits into two branches, one curving westward around the AH, the other eastward around the polar vortex. As air flows eastward around the polar vortex over the North Atlantic region, it rises. Flow of this nature is analogous to that observed in a mature baroclinic wave [*Thorncroft et al.*, 1993, Figure 1] and was observed by *Fairlie et al.* [1990] in their study of frontogenetic development during a sudden stratospheric warming (SSW). A SSW occurs when the AH and/or NAH are so robust that they dominate the polar vortex and turn the zonal mean wind poleward of 60°N easterly. The similarity between the structure of the AH-polar vortex pair and the classical tropospheric disturbances is notable. Other similarities include the westward tilt with altitude [*Harvey and Hitchman*, 1996] and evidence of narrow baroclinic zones [*Fairlie et al.*, 1990; *Pierce et al.*, 1993] in the stratosphere. Overlaid in both Figures 5a and 5b are boxes that depict the locations of the 13 SAM II soundings retrieved on January 23. Air is adequately sampled within the polar vortex and in the jet across the northern flank of the AH. Figure 5b shows that the locations of the SAM II soundings are colocated with where the isentropic surface is both the highest and the lowest in altitude. The extreme high-latitude location of the SAM II measurements made sampling the core of the AH challenging. SAM II sampled only the poleward flank of the AH during our case study. Fortunately, the Stratospheric Aerosol and Gas Experiment (SAGE) II instrument sampled
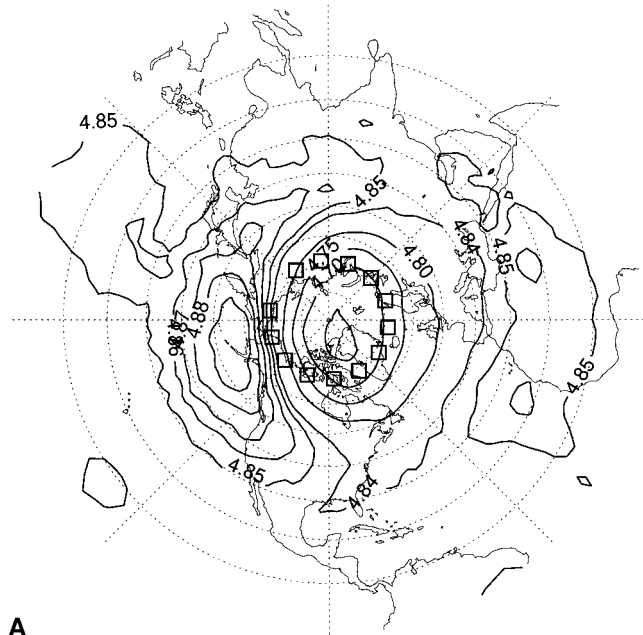
A
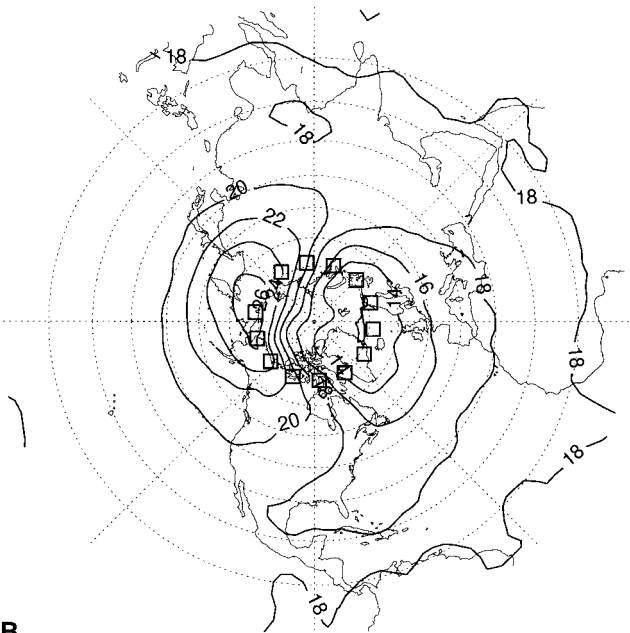
B

Figure 5. Northern Hemisphere polar stereographic on January 23 at 700 K of (a) Montgomery stream function and (b) pressure. (a) Montgomery stream function has been divided by 10^5 and the contour interval is 0.05 in the polar vortex decreasing to 0.01 in the anticyclones. (b) The contour interval is 2 hPa. (a, b) Boxes are overlaid, showing the locations of the January 23 SAM II soundings.

the AH domain on January 23, 1986. Magnitudes of SAGE II SADs near the center of the AH agree with those SAM II sampled on the poleward flank. This is expected since the AH recirculates and mixes air within it.

Figure 6 is a longitude-altitude section at 70°N on January 23 of M, where the zonal mean has been subtracted. This shows the vertical structure of the M field at the latitude of the SAM II measurements. As in Figure 2, the "wave 1" pattern above 550 K (about 21 km), with positive eddy M over the date
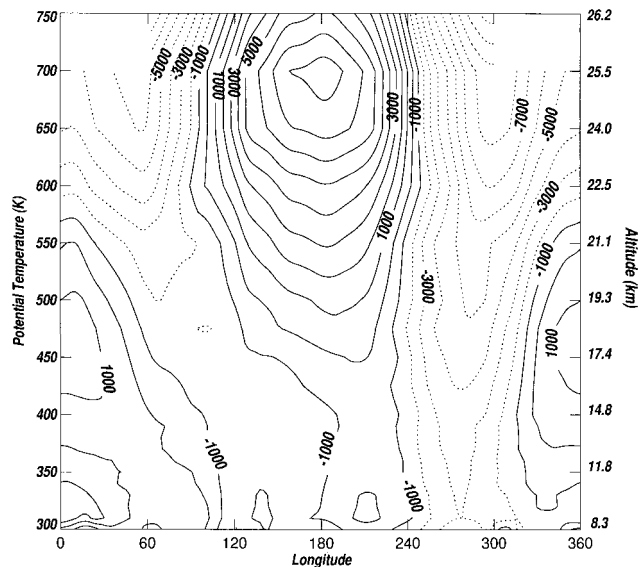

Figure 6. Longitude-altitude section at 70°N of eddy (deviation from the zonal mean) Montgomery stream function on January 23, 1986. Contour interval is 1000 m^2 s^{-2}.

line and negative over the GM, represents the AH and the polar vortex. The blank area in the polar vortex shows where the 750 K surface rises above 10 hPa, the highest ECMWF data level. The "wave 2" pattern of M below 550 K depicts an elongated polar vortex with two surrounding anticyclones, namely the downward extension of the AH and upward extension of the NAH. Figure 7 is a longitude-altitude cross section of SAM II SAD (% deviation from the zonal mean), at 69°N on the same day. It can be seen that the longitudinal structure in aerosol resembles that in the climatology (compare Figure 7 to Figure 3) with high aerosol in the anticyclones and low aerosol in the vortex (compare Figure 7 to Figure 6). The region
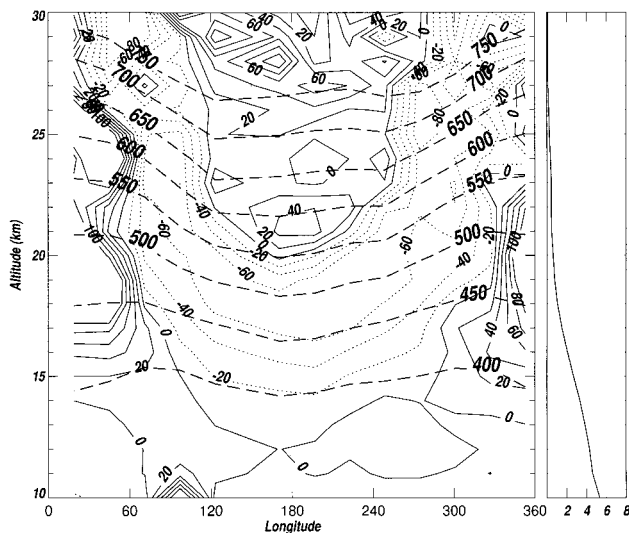

Figure 7. Longitude-altitude section of the percent deviation of SAD from the zonal mean at 69°N on January 23, 1986. Contour interval is 20%. Isentropic surfaces from 400–750 K by 50 K are dashed lines. Zonal mean SAD profile is given to the right in units of μm^2 cm^{-3}.
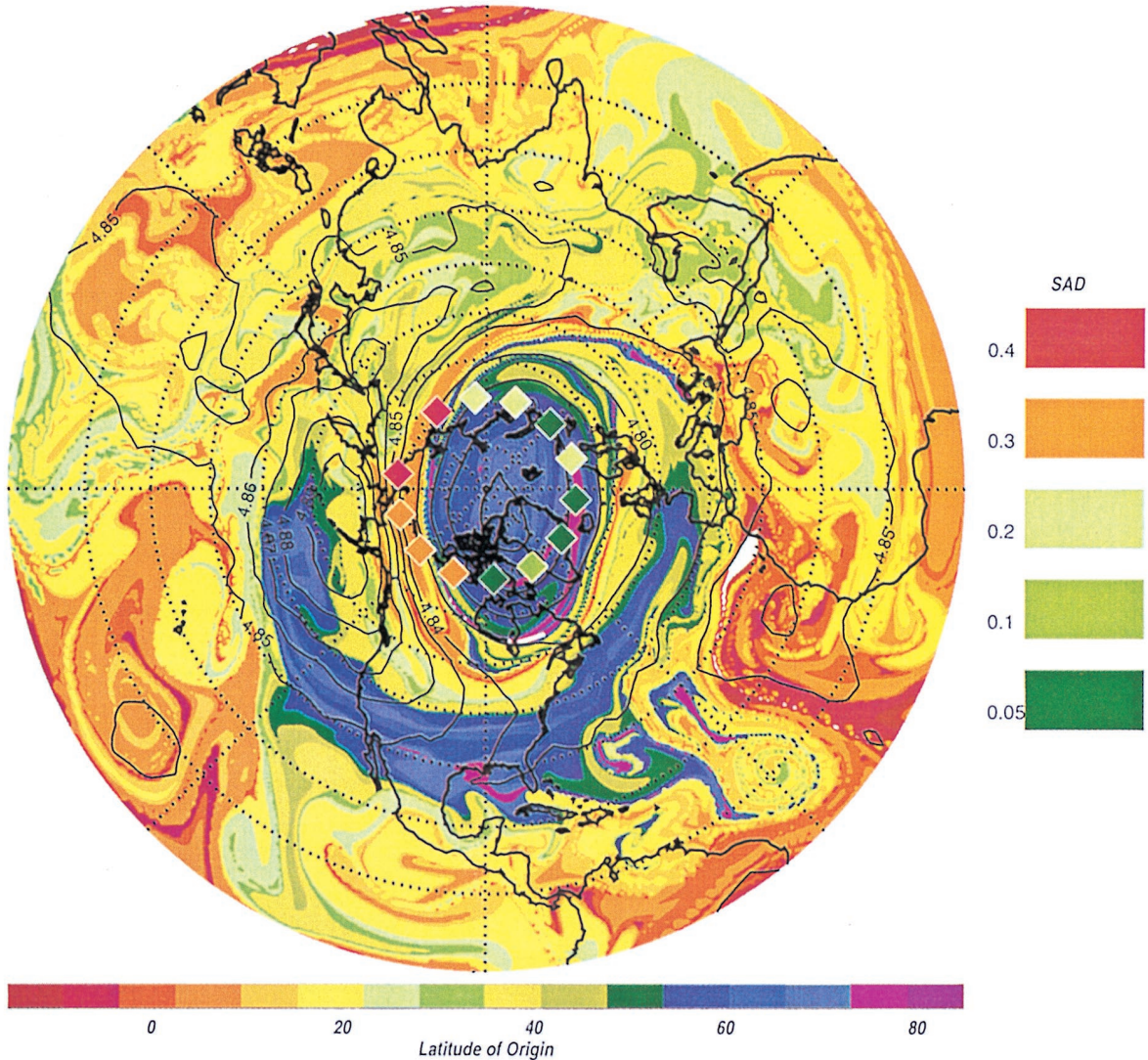
Plate 1. Northern Hemisphere polar stereographic of latitude of origin of 8-day back trajectories initialized at 0.5° by 0.5° resolution at 700 K on January 23, 1986. Montgomery stream function contours are overlaid in intervals of 1000 m² s⁻². Boxes are colored by their SAM II SAD values.

coincident with the AH shows a 20–60% increase in SAD over the zonal mean and over 100% increase in the NAH. The polar vortex is associated with regions which realize up to a 60% decrease in zonal mean aerosol. It is not surprising to find such an amplified pattern on daily timescales compared to the multiyear climatology. Absolute SAD values can be calculated from the zonal mean profile provided to the right of Figure 7. The isentropic levels from which we ran the back trajectories are superimposed. Henceforth analyses are described in isentropic coordinates.

In preparation for trajectory calculations, ECMWF winds and SAM II SADs are linearly interpolated to the following nine potential temperature surfaces: 450, 475, 500, 525, 550, 600, 650, 700, and 750 K. Trajectories are initialized on these vertically stacked layers at the times and locations of the SAM II soundings. Isentropic trajectories are then run backward in time to identify the origin of the high aerosol sampled in the AH. We use the NASA Langley trajectory model [*Pierce and Fairlie*, 1993; *Pierce et al.*, 1994] with a 20-min time step and

daily 0000 UT winds that are linearly interpolated in time and space to trajectory locations.

To more fully understand the global structure of intruding tropical air masses, we also initialize back trajectories on the same nine isentropic levels but on a 0.5° by 0.5° grid. On the last day of a trajectory calculation the latitudes of the trajectories (now irregularly spaced) are mapped back to the original grid on the first day. This popular and powerful technique is called reverse domain filling (RDF) [*Sutton et al.*, 1994], and while it does not in this case incorporate any aerosol information, it enables a high-resolution plot of latitude of origin to be constructed for comparison with aerosol measurements.

We initialize 8-day back trajectories on a 0.5° by 0.5° grid from 500 to 750 K beginning on January 23 in order to identify a source for the high aerosol in the AH. Plate 1 shows the 700 K latitude of origin of these trajectories on January 15. Air originating in the tropics is colored red, orange, and yellow. Midlatitude air is given by different shades of green, and air that originated at high latitudes is shown in blues and purples.

M contours, valid January 23, are overlaid to add context. Boxes represent SAM II measurements taken on January 23 and are colored by their SAD value. Notice the filament of tropical air stretched around the flank of the polar vortex into the vicinity of the AH. This low-latitude air originated over Africa, near the mobile anticyclone, and over the course of the trajectory was observed to surge poleward and eastward around the polar vortex. This filament is colocated with high SAD values, while low SAD values are found in the polar vortex. While we only show one isentropic surface, this high aerosol, low-latitude filament is visible down to 550 K, about 5 km lower, and can be thought of as an intruding "sheet" of air. This sheet has the same horizontal structure as that found in contour advection of the H_2SO_4 component of ISAMS aerosol [*Lambert et al.*, 1996]. In subsequent frames (not shown), part of this aerosol rich filament is advected westward and wraps up in the AH, while some continues on to be advected eastward around the polar vortex.

To identify the source region for the air that ends up in the AH, we initialized 515 trajectories inside the core of the AH at 700 K on January 23 and ran backward 8 days. Figures 8a and 8b are polar projections of M on 700 K on the first and last days of the back trajectories, respectively. Figure 8a shows the initialization of trajectories in the AH on January 23. Trajectories were initialized inside the 487,000 m^2 s^{-2} closed M contour. Figure 8b shows where the trajectories were 8 days earlier before the merger of the mobile anticyclone into the AH. Note that the AH migrated westward during the surge/merge event, a common feature. It is interesting that many of the trajectories were already in the AH and remained inside the anticyclone over the entire 8-day period. Most of the trajectories that originated elsewhere came from over Africa and from within the mobile anticyclone located north of the Persian Gulf. In addition, air appears to transit anticyclonically around a tropical disturbance over Africa and the Indian Ocean before getting swept poleward by the displaced polar jet (compare closed M contour over Africa in Figure 8a). During this time the African sector serves as the origin for AH air from 750 K down several kilometers to 650 K (not shown). The transport of air during this event represents a large influx of air into the AH from a discrete region, as opposed to air diffusing into the AH from middle latitudes. None of the trajectories originated deep inside the polar vortex.

To further explore the three-dimensional (3-D) structure of the intruding low-latitude air, we show the latitude of origin in a longitude-altitude section. Trajectories were initialized along a vertical section at 69°N, from 450 to 750 K and from the locations of the SAM II soundings on January 23. Similar to the previous high-resolution run, the trajectories were run backward 8 days. Figure 9 shows the latitude of origin of these trajectories. Source latitudes for the high aerosol sampled by SAM II (shown in Figure 7) are identified. Latitudes equatorward of 50°N are dashed. There is a broad and deep region in the AH, from 550 K to 750 K and from 120°E to 225°E, where the air originated equatorward of 30°N. Extension of the low-latitude intrusion above 750 K is likely but cannot be represented by the ECMWF data used here. Embedded within this region appear two cores of tropical air, at 120°E and 120°E, which originated from as far equatorward as 10°N. This air is in the polar jet and is coincident with the highest daily SAD values. This tropical source of the high aerosol air in the AH is consistent with previous trajectory analyses which also identify a tropical source for air in midlatitudes [*Waugh*, 1993; *O'Neill*
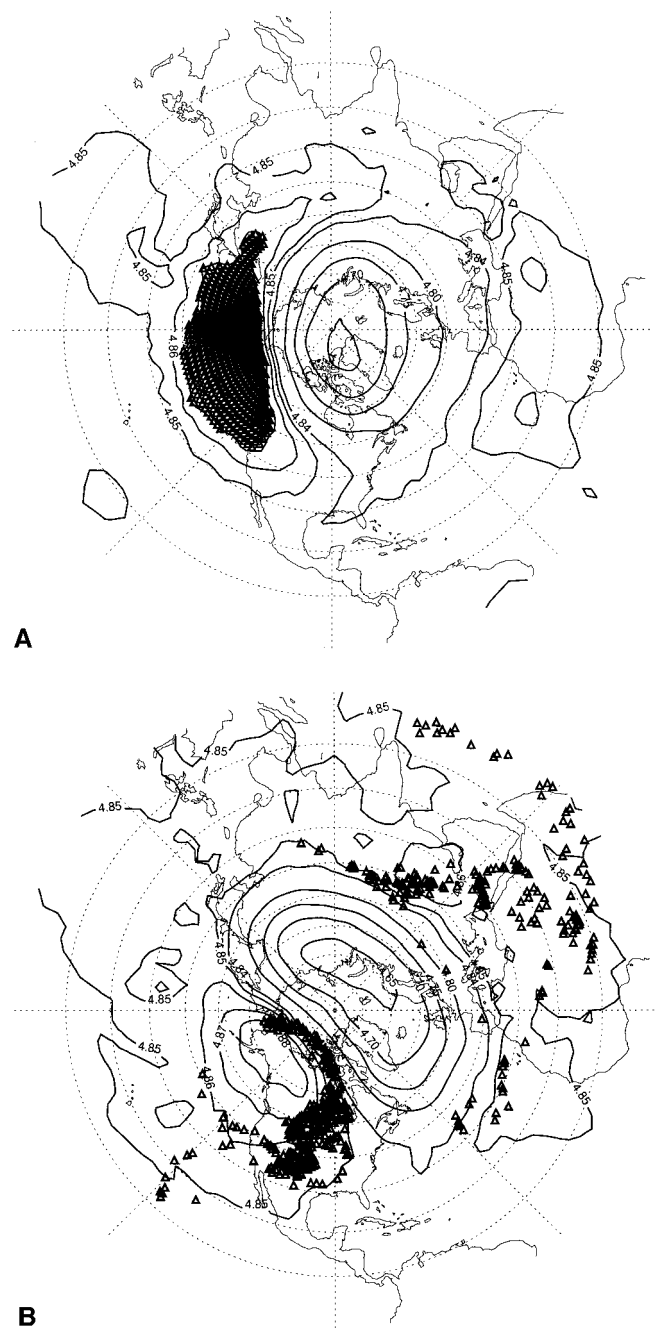
A

B

Figure 8. Northern Hemisphere polar stereographic of Montgomery stream function at 700 K on (a) January 23 (beginning of back trajectory) and (b) January 15 (end of back trajectory), 1986. Contour interval is as in Figure 5. (a) Triangles initialized in the AH on January 23. (b) Trajectory origins 8 days earlier on January 15.

et al., 1994; *Manney et al.*, 1995a, b; *Polvani et al.*, 1995; *Lambert et al.*, 1996]. Since these episodic poleward surges of tropical air occur repeatedly throughout the Northern Hemisphere winter, this case study is a step toward explaining the climatological high aerosol observed in the AH. In order to corroborate the SAM II aerosol measurements we looked for coincidences between the SAM II back trajectories and the in situ SAGE II soundings. Using a coincidence criteria of 5° longitude, 5° latitude, 50 K, and 6 hours, we found 121 coincidences.
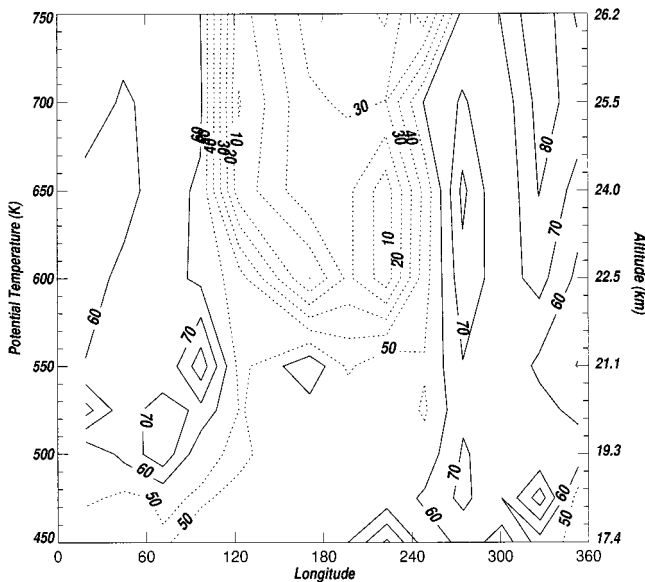
Figure 9. Longitude-altitude section at 69°N of latitude of origin of 8-day back trajectories which were initialized from SAM II soundings on January 23, 1986. Contour interval is 10° of latitude.

The corrolation coefficient between SAGE II and SAM II was 0.66, where SAGE II SADs were systematically higher than SAM II SADs. This difference is consistent with expected dillution of SAGE II aerosol along the SAM II back trajectory. Figure 9 does not suggest a tropical source for the high aerosol sampled over the GM (in Figure 7). We are uncertain as to the origin of the extreme values of SAD in this region. This air may have persisted in the mobile anticyclone or in the AH, and a longer trajectory may be needed to trace it back to the tropics. It could also be an increased signal due to PSCs. The corresponding longitude-altitude section of temperature on January 23 indicates temperatures less than 200 K above 50 hPa (about 500 K) over the GM, making PSC formation distinctly possible [*Poole and Pitts*, 1994].

5. Conclusions

Climatologically, high aerosol is observed in the AH. This result led us to investigate a mechanism that may act to maintain this structure and to identify a likely source for the climatological high aerosol in the AH. The trajectory analyses used in this case study illustrate the process whereby tropical high aerosol air is entrained into the AH. Back trajectories, initialized from both a 0.5° by 0.5° grid and from SAM II occultations on a day in which high aerosol was sampled in the AH, identify the air as having originated in the tropics. It was shown that the intruding aerosol rich air mass has a significant vertical range, extending from 550 K to at least 750 K (over 5 km deep). Moreover, it was found for this case study that the tropical source of high aerosol in the AH lies primarily in the African sector. Diffluence in the polar jet over Canada is likely to be a primary mechanism of mixing the tropical, high aerosol air throughout the hemisphere. Entrainment and detrainment along the path out of the tropics may be quantified with the techniques used here. Ongoing work includes quantifying mixing associated with poleward surges and evaluating implications for extratropical air mass types and deviations of tracer-

tracer plots from compact lines. The climatological frequency of anticyclonic surge events, such as considered here, needs to be determined to establish their role in the maintenance of the high aerosol in the AH and their contribution to exchange between the tropics and the midlatitudes.

References

Avallone, L. M., and M. Prather, Photochemical evolution of ozone in the lower tropical stratosphere, *J. Geophys. Res.*, *101*, 1457–1461, 1996.

Borrmann, S., J. E. Dye, D. Baumgardner, J. C. Wilson, H. H. Jonsson, C. A. Brock, M. Loewenstein, J. R. Podolske, G. V. Ferry, and K. S. Barr, In-situ measurements of changes in stratospheric aerosol and the N_2O-aerosol relationship inside and outside of the polar vortex, *Geophys. Res. Lett.*, *20*, 2559–2562, 1993.

Brewer, A. W., Evidence for a world circulation provided by the measurements of helium and water vapour distribution in the stratosphere, *Q. J. R. Meteorol. Soc.*, *75*, 351–363, 1949.

Chen, P., J. R. Holton, A. O'Neill, and R. Swinbank, Isentropic mass exchange between the tropics and extratropics in the stratosphere, *J. Atmos. Sci.*, *51*, 3006–3018, 1994.

Dahlberg, S. P., and K. P. Bowman, Climatology of large-scale isentropic mixing in the Arctic winter stratosphere from analyzed winds, *J. Geophys. Res.*, *99*, 20,585–20,599, 1994.

Dameris, M., M. Wirth, W. Renger, and V. Grewe, Definition of the polar vortex edge by LIDAR data of the stratospheric aerosol: A comparison with values of potential vorticity, *Beitr. Phys. Atmos.*, *68*(2), 113–119, 1995.

Danielsen, E. F., Stratospheric-tropospheric exchange based upon radioactivity, ozone, and potential vorticity, *J. Atmos. Sci.*, *25*, 502–518, 1968.

Fairlie, T. D. A., Three-dimensional transport simulations of the dispersal of volcanic aerosol from Mount Pinatubo, *Q. J. R. Meteorol. Soc.*, *121*, 1943–1980, 1995.

Fairlie, T. D. A., M. Fisher, and A. O'Neill, The development of narrow baroclinic zones and other small-scale structure in the stratosphere during simulated major warmings, *Q. J. R. Meteorol. Soc.*, *116*, 287–315, 1990.

Grant, W. B., E. V. Browell, C. S. Long, L. L. Stowe, R. G. Granger, and A. Lambert, Use of volcanic aerosols to study the tropical stratospheric reservoir, *J. Geophys. Res.*, *101*, 3973–3988, 1996.

Hamill, P., E. J. Jensen, P. B. Russell, and J. J. Bauman, The life cycle of stratospheric aerosol particles, *Bull. Am. Meteorol. Soc.*, *78*(7), 1395–1410, 1997.

Harvey, V. L., A climatology of the Aleutian High, 118 pp., M.S. thesis, Univ. of Wisconsin, Madison, 1994.

Harvey, V. L., and M. H. Hitchman, A climatology of the Aleutian High, *J. Atmos. Sci.*, *53*, 2088–2101, 1996.

Hitchman, M. H., M. McKay, and C. R. Trepte, A climatology of stratospheric aerosol, *J. Geophys. Res.*, *99*, 20,689–20,700, 1994.

Hofmann, D. J., and S. J. Oltmans, Anomalous Antarctic ozone during 1992: Evidence for Pinatubo volcanic aerosol effects, *J. Geophys. Res.*, *98*, 18,555–18,561, 1993.

Holton, J. R., and H.-C. Tan, The influence of the equatorial quasi-biennial oscillation on the global circulation at 50 mb, *J. Atmos. Res.*, *37*, 2200–2208, 1980.

Holton, J. R., P. H. Haynes, M. E. McIntyre, A. R. Douglass, R. R. Rood, and L. Pfister, Stratospheric-tropospheric exchange, *Rev. Geophys.*, *33*, 403–439, 1995.

Kent, G. S., C. R. Trepte, U. O. Farrukh, and M. P. McCormick, Variation in the stratospheric aerosol associated with the north cyclonic polar vortex as measured by the SAM II satellite sensor, *J. Atmos. Sci.*, *42*, 1536–1551, 1985.

Knox, J. A., A theoretical and observational study of inertial instability and nonlinear balance, 351 pp., Ph.D. thesis, Univ. of Wisconsin, Madison, 1996.

Kumer, J. B., J. L. Merganthaler, and A. E. Roche, CLAES CH_4, N_2O,

and CCL$_2$F$_2$ (F12) global data, *Geophys. Res. Lett.*, *20*, 1239–1242, 1993.

Lahoz, W. A., et al., Northern hemisphere mid-stratosphere vortex processes diagnosed from H$_2$O, N$_2$O and potential vorticity, *Geophys. Res. Lett.*, *20*, 2671–2674, 1993.

Lahoz, W. A., et al., Three-dimensional evolution of water vapour distributions in the northern hemisphere stratosphere as observed by the Microwave Limb Sounder, *J. Atmos. Sci.*, *51*, 2914–2930, 1994.

Lambert, A. R. G. Grainger, H. L. Rogers, W. A. Norton, C. D. Rodgers, and F. W. Taylor, The H$_2$SO$_4$ component of stratospheric aerosols derived from satellite infrared extinction measurements: Application to stratospheric transport studies, *Geophys. Res. Lett.*, *23*, 2219–2222, 1996.

Langford, A. O., T. J. O'Leary, and M. H. Hitchman, Transport of the Pinatubo volcanic aerosol to a northern midlatitude site, *J. Geophys. Res.*, *100*, 9007–9016, 1995.

Leovy, C. B., C.-R. Sun, M. H. Hitchman, E. E. Remsberg, J. M. Russell, L. L. Gordley, J. C. Gille, and L. V. Lyjak, Transport of ozone in the middle stratosphere: Evidence for planetary wave breaking, *J. Atmos. Sci.*, *42*, 230–244, 1985.

Manney, G. L., L. Froidevaux, J. W. Waters, L. S. Elson, E. F. Fishbein, R. W. Zurek, R. S. Harwood, W. A. Lahoz, The evolution of ozone observed by UARS MSL in the 1992 late winter southern polar vortex, *Geophys. Res. Lett.*, *20*, 1279–1282, 1993.

Manney, G. L., R. W. Zurek, A. O'Neill, and R. Swinbank, On the motion of air through the stratospheric polar vortex, *J. Atmos. Sci.*, *51*, 2973–2994, 1994.

Manney, G. L., L. Froidevaux, J. W. Waters, R. W. Zurek, J. C. Gille, J. B. Kumer, J. L. Merganthaler, A. E. Roche, A. O'Neill, and R. Swinbank, Formation of low-ozone pockets in the middle stratospheric anticyclone during winter, *J. Geophys. Res.*, *100*, 13,939–13,950, 1995a.

Manney, G. L., et al., Lagrangian transport calculations using UARS data, I, Passive tracers, *J. Atmos. Sci.*, *52*, 3049–3068, 1995b.

McCormick, M. P., and R. E. Veiga, SAGE II measurements of early Pinatubo aerosols, *Geophys. Res. Lett.*, *19*, 155–158, 1992.

McCormick, M. P., P. Hamil, T. J. Pepin, W. P. Chu, T. J. Swissler, and L. R. McMaster, Satellite studies of the stratospheric aerosol, *Bull. Am. Meteorol. Soc.*, *60*, 1038–1046, 1979.

Mecikalski, J. R., and G. J. Tripoli, Inertial available kinetic energy and the dynamics of tropical plume formation, *Mon. Weather Rev.*, *126*, 2200–2216, 1998.

Minschwaner, K., A. E. Dessler, J. W. Elkins, C. M. Volk, D. W. Fahey, M. Loewenstein, J. R. Podolske, A. E. Roche, and K. R. Chan, Bulk properties of isentropic mixing into the tropics in the lower stratosphere, *J. Geophys. Res.*, *101*, 9433–9439, 1996.

Mote, P. W., K. H. Rosenlof, M. E. McIntyre, E. S. Carr, J. C. Gille, J. R. Holton, J. S. Kinnersley, H. C. Pumphrey, J. M. Russell III, and J. W. Waters, An atmospheric tape recorder: The imprint of tropical tropopause temperatures on stratospheric water vapor, *J. Geophys. Res.*, *101*, 3989–4006, 1996.

Murphy, D. M., D. W. Fahey, and M. H. Proffitt, Reactive nitrogen and its correlation with ozone in the lower stratosphere and upper troposphere, *J. Geophys. Res.*, *98*, 8751–8773, 1993.

Norton, W. A., Breaking Rossby waves in a model stratosphere diagnosed by a vortex-following coordinate system and a technique for advecting material contours, *J. Atmos. Sci.*, *51*, 654–673, 1994.

O'Neill, A., V. D. Pope, W. L. Grose, M. Bailey, H. MacLean, and R. Swinbank, Evolution of the stratosphere during northern winter 1991–92 as diagnosed from UKMO analyses, *J. Atmos. Sci.*, *51*, 2800–2817, 1994.

Orsolini, Y., On the formation of ozone laminae at the edge of the Arctic polar vortex, *Q. J. R. Meteorol. Soc.*, *121*, 1923–1941, 1995.

Orsolini, Y. J., G. Hansen, U-P. Hoppe, G. L. Manney, and K. H. Fricke, Dynamical modelling of wintertime lidar observations in the Arctic: Ozone laminae and ozone depletion, *Q. J. R. Meteorol Soc.*, *123*, 785–800, 1997.

O'Sullivan, D., and T. J. Dunkerton, The influence of the quasi-biennial oscillation on global constituent distributions, *J. Geophys. Res.*, *102*, 21,731–21,743, 1997.

O'Sullivan, D., and M. H. Hitchman, Inertial instability and Rossby wave breaking in a numerical model, *J. Atmos. Sci.*, *49*, 991–1002, 1992.

Pierce, R. B., and T. D. A. Fairlie, Chaotic advection in the stratosphere: Implications for the dispersal of chemically perturbed air from the polar vortex, *J. Geophys. Res.*, *98*, 18,589–18,595, 1993.

Pierce, R.-B., W. T. Blackshear, T. D. Fairlie, W. L. Grose, and R. E. Turner, The interaction of radiative and dynamical processes during a simulated sudden stratospheric warming, *J. Atmos. Sci.*, *50*, 3829–3851, 1993.

Pierce, R. B., T. D. A. Fairlie, W. L. Grose, R. Swinbank, and A. O'Neill, Mixing processes within the polar night jet, *J. Atmos. Sci.*, *51*, 2857–2972, 1994.

Plumb, R. A., D. W. Waugh, R. J. Atkinson, P. A. Newman, L. R. Lait, M. R. Schoeberl, E. V. Browell, A. J. Simmons, and M. Loewenstein, Intrusions into the lower stratosphere Arctic vortex during the winter of 1991–1992, *J. Geophys. Res.*, *99*, 1089–1105, 1994.

Polvani, L. M., D. W. Waugh, and R. A. Plumb, On the subtropical edge of the stratospheric surf zone, *J. Atmos. Sci.*, *52*, 1288–1309, 1995.

Poole, L. R., and M. C. Pitts, Polar stratospheric cloud climatology based on Stratospheric Aerosol Measurement II observations from 1978 to 1989, *J. Geophys. Res.*, *99*, 13,083–13,089, 1994.

Postel, G. A., and M. H. Hitchman, A climatology of Rossby wave breaking along the subtropical tropopause, *J. Atmos. Sci.*, *55*, in press, 1998.

Randel, W. J., J. C. Gille, A. E. Roche, J. B. Kumer, J. L. Merganthaler, J. W. Waters, E. F. Fishbein, and W. A. Lahoz, Stratospheric transport from the tropics to middle latitudes by planetary-wave mixing, *Nature*, *365*, 533–535, 1993.

Rogers, H. L., W. A. Lambert, and R. G. Granger, Transport of Mt. Pinatubo aerosol by tropospheric synoptic-scale waves, *Q. J. R. Meteorol. Soc.*, *124*, 193–209, 1998.

Rom-Kedar, V., and N. Paldor, From the tropics to the poles in forty days, *Bull. Am. Meteorol. Soc.*, *78*, 2779–2784, 1997.

Rood, R., A. Douglass, and C. Weaver, Tracer exchange between tropics and middle latitudes, *Geophys. Res. Lett.*, *19*, 805–808, 1992.

Rosen, J. M., N. T. Kjome, and H. Fast, Penetration of Mt. Pinatubo aerosols into the north polar vortex, *Geophys. Res. Lett.*, *19*, 1751–1754, 1992.

Russell, P. B., et al., Satellite and correlative measurements of the stratospheric aerosol, II, Comparison of measurements made by SAM II, dustsondes and an airborne lidar, *J. Atmos. Sci.*, *38*, 1295–1312, 1981.

Schoeberl, M. R., and P. A. Newman, A multiple-level trajectory analysis of vortex filaments, *J. Geophys. Res.*, *100*, 25,801–25,815, 1995.

Schoeberl, M. R., L. R. Lait, P. A. Newman, and J. E. Rosenfield, The structure of the polar vortex, *J. Geophys. Res.*, *97*, 7859–7882, 1992.

Schoeberl, M. R., A. E. Roche, J. M. Russell III, D. Ortland, P. B. Hays, and J. W. Waters, An estimation of the dynamical isolation of the tropical lower stratosphere using UARS wind and trace gas observations of the quasi-biennial oscillation, *Geophys. Res. Lett.*, *24*, 53–56, 1997.

Shapiro, M. A., R. C. Schnell, F. P. Parungo, S. J. Oltmans, and B. A. Bodhaine, El Chichon volcanic debris in an Arctic tropause fold, *Geophys. Res. Lett.*, *11*, 421–424, 1984.

Stolarski, R. S., et al., 1995 Scientific assessment of the atmospheric effects of stratospheric aircraft, *NASA Ref. Publ. 1381*, 64 pp., 1995.

Sutton, R. T., H. Maclean, R. Swinbank, A. O'Neill, and F. W. Taylor, High-resolution stratospheric tracer fields estimated from satellite observations using Lagrangian trajectory calculations, *J. Atmos. Sci.*, *51*, 2995–3005, 1994.

Thomason, L. W., L. R. Poole, and T. Deshler, A global climatology of stratospheric aerosol surface area density deduced from Stratospheric Aerosol and Gas Experiment II measurements: 1984–1994, *J. Geophys. Res.*, *102*, 8967–8976, 1997.

Thorncroft, C. D., B. J. Hoskins, and M. E. McIntyre, Two paradigms of baroclinic-wave life-cycle behaviour, *Q. J. R. Meteorol. Soc.*, *119*, 17–55, 1993.

Trenberth, K. E., Global analyses from ECMWF and atlas of 1000 to 10 mb circulation statistics, *NCAR Tech. Note, NCAR/TN-373+STR*, Natl. Cent. for Atmos. Res., Boulder, Colo., 1992.

Trepte, C. R., and M. H. Hitchman, Tropical stratospheric circulation deduced from satellite aerosol data, *Nature*, *355*, 626–628, 1992.

Trepte, C. R., R. E. Veiga, and M. P. McCormick, The poleward dispersal of Mount Pinatubo volcanic aerosol, *J. Geophys. Res.*, *98*, 18,563–18,573, 1993.

Volk, C. M., et al., Quantifying transport between the tropical and mid-latitude lower stratosphere, *Science*, *272*, 1763–1768, 1996.

Waugh, D. W., Subtropical stratospheric mixing linked to disturbances in the polar vortices, *Nature*, *365*, 535–537, 1993.

Waugh, D. W., Seasonal variation of isentropic transport out of the tropical stratosphere, *J. Geophys. Res*., *101*, 4007–4023, 1996.

Waugh, D. W., R. A. Plumb, P. A. Newman, M. R. Schoeberl, L. R. Lait, M. Loewenstein, J. R. Podolske, J. W. Elkins, and K. R. Chan, Fine-scale, poleward transport of tropical air during AASE 2, *Geophys. Res. Lett*., *21*, 2603–2606, 1994.

Ziemke, J. R., and J. L. Stanford, Zonal asymmetries in SAMS stratospheric methane and nitrous oxide, *Q. J. R. Meteorol. Soc*., *121*, 911–925, 1995.

T. D. Fairlie, V. L. Harvey, and R. B. Pierce, NASA Langley Research Center, MS 401B, Hampton, VA 23681. (v.1.harvey@larc.nasa.gov)

M. H. Hitchman, Department of Atmospheric and Oceanic Sciences, University of Wisconsin-Madison, Madison, WI 53706.